Brazilian Journal of Physics
ISSN: 0103-9733
luizno.bjp@gmail.com
Sociedade Brasileira de Física
Brasil

Pereyra, I.; Villacorta, C. A.; Carreño, M.N.P.; Prado, R.J.; Fantini, M.C.A.
Highly Ordered Amorphous Silicon-Carbon Alloys Obtained by RF PECVD
Brazilian Journal of Physics, vol. 30, núm. 3, septiembre, 2000, pp. 533-540
Sociedade Brasileira de Física
Sâo Paulo, Brasil

Available in: http://www.redalyc.org/articulo.oa?id=46413500009

- How to cite
- Complete issue
- More information about this article
- Journal's homepage in redalyc.org

Scientific Information System
Network of Scientific Journals from Latin America, the Caribbean, Spain and Portugal
Non-profit academic project, developed under the open access initiative

Highly Ordered Amorphous Silicon-Carbon Alloys Obtained by RF PECVD

I. Pereyra, C. A. Villacorta, M.N.P. Carreño,
Depto. de Eng. Sistemas Eletrônicos, Escola Politécnica,
Universidade de São Paulo, São Paulo, Brasil

R.J. Prado, and M.C.A. Fantini
Instituto de Física, Universidade de São Paulo, São Paulo, Brasil

Received 15 February, 2000; received in final form on 29 March, 2000

We have shown that close to stoichiometry RF PECVD amorphous silicon carbon alloys deposited under silane starving plasma conditions exhibit a tendency towards c-SiC chemical order. Motivated by this trend, we further explore the effect of increasing RF power and H_2 dilution of the gaseous mixtures, aiming to obtain the amorphous counterpart of c-SiC by the RF-PECVD technique. Doping experiments were also performed on ordered material using phosphorus and nitrogen as donor impurities and boron and aluminum as acceptor ones. For nitrogen a doping efficiency close to device quality a-Si:H was obtained, the lower activation energy being 0,12 eV with room temperature dark conductivity of 2.10^{-3} (Ω.cm). Nitrogen doping efficiency was higher than phosphorous for all studied samples. For p-type doping, results indicate that, even though the attained conductivity values are not device levels, aluminum doping conducted to a promising shift in the Fermi level. Also, aluminum resulted a more efficient acceptor than boron, in accordance to observations in crystalline SiC material.

I Introduction

The deposition of amorphous hydrogenated silicon carbide thin films, a-$Si_{1-x}C_x$:H, by PECVD has been extensively studied due to the ability of this technique to control the carbon content in the films and, therefore, the optical gap (E_o). The increase in the optical gap, following the increase in the carbon concentration, is desirable for many device strategies and has been one of the main appeals of these alloys. However, for high carbon content films ($x \sim 0.5$), a decrease in the optical gap is generally observed, which leads to a difficulty in obtaining a material with $E_o > 2,5 - 3$ e V [1]. This decrease in the optical gap observed for carbon rich a-$Si_{1-x}C_x$:H has been related to the existence of graphite-like sp^2 C-C bonding instead of diamond-like sp^3 C-C bonding [1,2].

Solomon and co-workers [3] showed that in the low power regime, where the RF power is sufficient to break the SiH_4 molecules but not the CH_4 ones, the presence of graphite-like bonds is avoided. However the carbon to silicon relative concentration in the solid phase is limited up to 50% and the resulting material is rich in methylated radicals. Recently, we have demonstrated that it is possible to obtain non methylated PECVD a-SiC:H thin films (from $SiH_4 + CH_4$) with carbon to silicon ratio higher than 0.5 (up to 0.7) with C-C bonds occurring mainly in the sp^3 (diamond-like) hybridization, optical gap as high as 3.7 eV and high electrical resistivity [4-6]. The results demonstrate that these diamond-like silicon carbide films are obtained in a special deposition condition, called "silane starving plasma" regime [6]. This regime is a particular case of the low power density one where, for a critically low SiH_4 flow, the film growth is controlled by the spare SiH_4 radicals, simplifying the plasma chemistry and promoting carbon incorporation in the sp^3 hybridization. In this way we have shown that the starving plasma deposition conditions have a crucial role in the growth of close to stoichiometry material exhibiting a tendency towards the chemical order of crystalline silicon carbide, this is to say each silicon atom (tetrahedrally) bonded to four carbon atoms and each carbon atom bonded to four silicon atoms. For carbon rich samples this deposition regime promotes the production of films with very high values of the optical gap, strongly suggesting the incorporation of carbon in sp^3 bonds.[1]

Chemical order in silicon carbon alloys has been a controversial point. Cardona et. al. in their pioneering work [7], and many authors after them, argued that silicon and carbon atoms are randomly distributed, with no preferential hetero-nuclear (Si-C) bonds. On the other hand, Evangelisti et al.[8] have reported a strong tendency towards the chemical order of c-SiC in a-$Si_{1-x}C_x$:H films. Our work indicates that material grown in the low power regime out of silane starving conditions are silicon rich randomly distributed while the material grown with silane starving plasma conditions is close to stoichiometry or carbon rich and exhibits a preference for hetero-nuclear bonding (SiC chemical order).

Encouraged by the chemical order exhibited by a-$Si_{1-x}C_x$:H alloys produced in the silane starving regime we further explore the possibility of increasing even more the chemical order to promote the growth of an amorphous counterpart of c-SiC or even SiC microcrystals (μ-SiC). We also analyze the n and p type doping efficiency of these a-$Si_{1-x}C_x$:H films.

It is known that hydrogen etching during the growth of amorphous silicon has a very important effect on the structural properties of a-Si:H films [9] and H_2 dilution of the gas mixture is a technique widely used to produce microcrystalline Si. In this way, some authors have used hydrogen dilution and higher RF power density to produce microcrystalline p-type silicon carbon (boron doped) alloys. In fact they obtained silicon micro-crystals embedded in an hydrogenated amorphous silicon carbon alloy network [10,11]. At the present time, to our knowledge, there is no report of SiC micro-crystals obtained by RF-PECVD which justifies our interest in pursuing this task taking advantage of the promising properties of the a-SiC:H obtained in silane starving plasma conditions.

Similarly, the structural order in a-SiC:H grown in "silane starving plasma" regime is a very important characteristic for doping experiments, since it is an universal fact that amorphous silicon based alloys exhibit an enhanced degree of disorder for increasing alloy element content, which decreases the carrier mobility and prevents the occurrence of an efficient doping, limiting their device applications. In this way we study the influence of the chemical order, induced by the "starving plasma" condition on the n-type and p-type doping efficiency of PECVD a-$Si_{1-x}C_x$:H.

II Experimental details

a-$Si_{1-x}C_x$:H films were prepared by the radio frequency (RF) Plasma Enhanced Chemical Vapor Deposition (PECVD) technique, with an RF frequency of 13,56 MHz, from appropriated gaseous mixtures of SiH_4 + CH_4 + H_2 in a capacitively coupled reactor. A more detailed description of the deposition system can be found elsewhere [12]. RF power density, methane concentration, and hydrogen dilution of the gaseous mixtures were varied. Substrate temperature for all the samples was 300 ^{o}C and silane flow was kept at the minimum value (3 sccm) in order to guarantee the "starving regime".

To establish the role of the "starving plasma" in the doping efficiency of a-SiC:H, the first experiments were carried out to compare the performance of samples grown in and out of this condition. For this purpose, both types of samples were ion-implanted with $3 \cdot 10^{20}\text{cm}^{-3}$ phosphorous and nitrogen. More details on the ion-implantation are reported elsewhere [13].

Based on the results obtained for samples grown with H_2 dilution of the gaseous mixture and on n-type doping, in case of the p-type doping experiments we centered on samples grown in "silane starving plasma" with H_2 dilution. Since good results in crystalline SiC have been obtained with aluminum, we utilized this doping element as acceptor impurity. However this impurity had to be introduced in the films through low temperature thermal diffusion experiments due to technical difficulties with the aluminum ion implantation. Aluminum diffusion was carried out by thermally evaporating a thin aluminum layer followed by a thermal annealing step. The analyzed annealing steps were 350 ^{o}C for 4, 8 and 12 hours and 450 ^{o}C for 0, 5, 2, 4 and 6 hours.

The films structure and bonding were characterized by Fourier transform infrared (FTIR) spectroscopy, optical absorption and extended X-ray absorption fine structure (EXAFS). The atomic concentrations of Si, C, N and P were determined by Rutherford backscattering (RBS) using a 2.3 MeV He^+ beam, with scattering angle of 170^o. The H content was determined through forward recoil spectrometry (FRS) with a target tilt angle of 75^o and 30^o detection angle. The transport properties of doped samples were studied analyzing the thermal dependence of the dark conductivity, $\sigma_d(T)$, measured in a vacuum cryostat. The thermal activation energy (E_a) was determined from the Arrhenius plot. In those plots the data were fitted with a function $\ln[\sigma_d(T)] = A + B/T$ and the activation energy was obtained from the slopes of those functions. The reproducibility of these results lead to an estimated error less than 10% for the conductivity. A 10% error for the activation energy was obtained by comparison of the maximum and minimum slopes in the Arrhenius plot.

III Results and discussion

III.1. H_2 Dilution and RF power

Fig. 1 shows the optical gap E_o as a function of CH_4 concentration for samples grown under starving plasma conditions with and without hydrogen diluted gaseous mixtures. It is observed that for samples grown without H_2 dilution the optical band gap increases slowly for CH_4 concentration values up to around 77%, while for higher concentration values it increases abruptly up to values higher than 3 eV. Samples deposited with

H_2 dilution show a similar but more pronounced behavior, the transition occurring at higher values of the CH_4 concentration (approximately 88%). This transition is associated with the passage over the stoichiometric composition ($x = 0.5$), so these results suggest a lower carbon incorporation in the solid phase for hydrogen diluted deposited material.

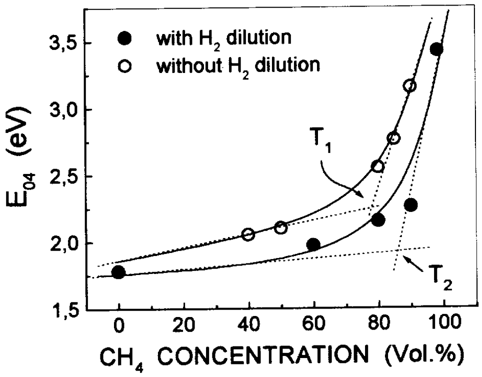

Figure 1. Optical gap as a function of the methane concentration for samples deposited at a RF power density of $25 mW/cm^2$ and with a H_2 flow of 100 sccm (•) and without H_2 dilution (∘).

In Fig.2 the integrated absorption of the IR absorption peak at 780 cm^{-1}, assigned to the Si-C stretching vibrations [1], divided by the sample thickness as function of methane volume fraction is depicted, for the same samples in Fig. 1. A maximum in the integrated absorption is observed for both sets of samples. However the peak position is shifted towards higher CH_4 concentrations for the H_2 diluted samples. Actually this maximum is an indication that the stoichiometric concentration x=0.5 has been passed through, since for higher carbon content the density of Si-C bonds should decrease and the C-C bonds should increase. In this way this result indicates, in accordance with the RBS measurements and the optical gap results, that stoichiometry is attained for higher CH_4 concentrations for samples deposited with H_2 diluted gas mixtures. For samples prepared at 25 mW/cm^2 and with H_2 dilution no traces, within the detection limit of ~1% of the FTIR technique, of CH_n bonds are observed. The concentration of SiH_n is also lower than in films grown without H_2 dilution and becomes very small for a CH_4 concentration of 98%. This means that for increasing C content in the solid phase, the polymeric phase always present in the hydrogenated amorphous silicon carbon alloys has been almost eliminated by the "etching process" and very low hydrogen content is obtained.

Having identified the methane concentration leading to close to stoichiometry material for hydrogen diluted gaseous mixtures and a RF power of 25 mW/cm^2, we chose this condition to perform our studies on the effect of increasing H_2 dilution and RF power densities on the structural properties of the films.

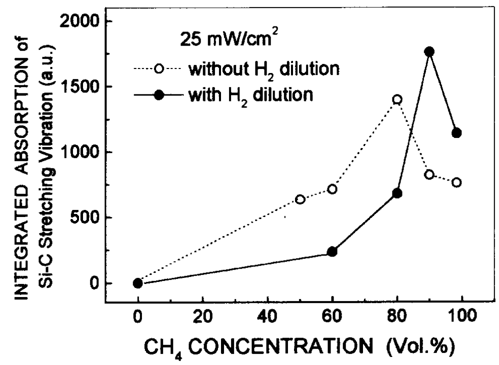

Figure 2. Integrated absorption intensity for the Si-C bond vibration peak vs. methane concentration for samples deposited at a RF power density of $25 mW/cm^2$ with a H_2 flow of 100 sccm (•) and without H_2 dilution (∘).

In Table 1 the RBS results are summarized. It is observed that increasing RF power increases the carbon content and decreases the hydrogen concentration of the films, increasing hydrogen flow decreased the hydrogen content even further.

Table 1: Composition of the studied samples obtained from RBS measurements.

Power density (mW/cm^2)	**H_2 flow (sccm)**	**H (at.%)**	**C (at.%)**	**Si (at.%)**	**x**
50	0	0.54	0.28	0.15	0.64
12.5	100	0.33	0.26	0.34	0.32
50	100	0.33	0.26	0.36	0.35
75	100	0.27	0.36	0.34	0.46
125	100	0.26	0.38	0.33	0.49
12.5	200	0.20	0.28	0.44	0.32
12.5	300	0.20	0.28	0.42	0.35

The FTIR spectra for samples grown with different H_2 flow, depicted in Fig. 3 show an enhanced absorption band at 780 cm^{-1}. Since the sample deposited without hydrogen dilution and 90% methane volume concentration is carbon rich as indicated by the RBS measurements [14] the increase in the Si-C band can be attributed to the fact that the samples are getting closer to stoichiometry, indicating that the H_2 etching process attacks preferentially carbon bonds. This hypothesis is confirmed by RBS measurements, which show that the Si/C ratio increases for increasing H_2 dilution. At the same time, the CH_n and the Si-CH_n stretching vibration absorption bands (in the 2800 cm^{-1} to 3000 cm^{-1} and 1250 to 1350 cm^{-1} spectral regions, respectively) decrease and for H_2 flow higher than 100 sccm and the CH_n related bands disappear which is also consistent with the hypothesis of preferential carbon etching. The FTIR spectra also show a pronounced decrease in the H content of the films for increasing H_2 flow, revealed by the CH_n and SiH_n bonding configurations. It is also observed that the Si-H stretching absorption band located at 2090 cm^{-1}, decreases but it does not disappear as the CH_n bands, which is consistent with the hypothesis of preferential etching of the C-H bonds.

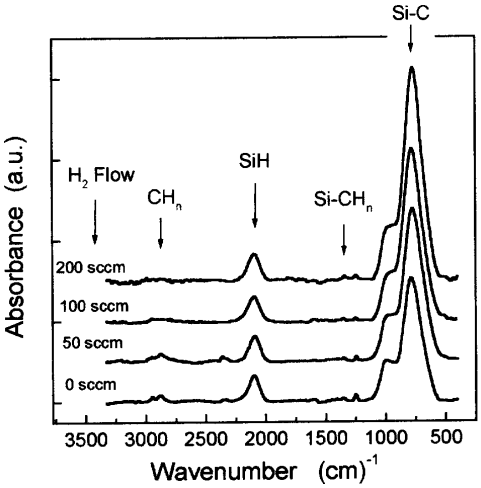

Figure 3. Infrared spectra for samples deposited with a RF power density of 25mW/cm^2, 90% methane volume fraction and varying H_2 flow.

In order to study the effect of increasing RF power densities a sample set, varying the RF power density between 12,5 and 500 mW/cm^2 and keeping constant all the other deposition parameters, was prepared. It was also found that, as the RF power density increases, the deposition rate increases. This result indicates that for higher RF power the deposition mechanism increases more rapidly than the etching one. In Fig. 4 an increase in the Si-C absorption band for increasing RF power densities, up to 250 mW/cm^2, is observed. However further increase up to 500 mW/cm^2 decreases the amplitude of this band. This result is interpreted as due to an increasing carbon concentration in the samples. For low RF power the samples are silicon rich while for high RF power carbon rich samples are obtained. The maximum in the Si-C absorption band obtained for 250 mW/cm^2 indicates that for these deposition parameters very close to stoichiometry material is produced. The observed increase in the carbon content of the samples, also supported by the RBS measurements and by the increasing CH_n related bands, indicates that for high RF power the etching mechanism is less efficient in extracting the C-H bonds. This last result is consistent with the observed increase in the deposition rate.

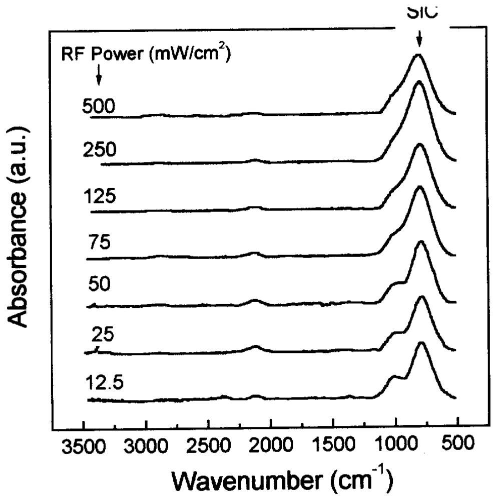

Figure 4. Infrared spectra for samples deposited with a H_2 flow of 100 sccm, 90% methane volume fraction and varying the RF power density.

From the EXAFS data at the Si K edge it was possible to analyze the short range structural and chemical order of the films. Assuming that the material is a binary alloy, composed of Si and C atoms, which is valid due to the low oxygen contamination (~ 1% - 3%), the coordination of carbon atoms with silicon was estimated [15].

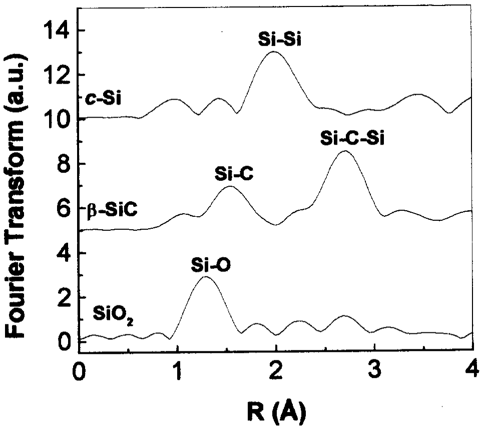

Figure 5. Fourier transform of the EXAFS spectra for the reference samples.

Fig. 5 presents the Fourier transform of the EXAFS spectra for the reference samples (SiO_2, c-Si and

β-SiC), showing the characteristic peaks. Due to the phase-shift, the apparent bonding distances are about 1.15 Å for Si-O, 1.6 Å for Si-C and 2.0 Å for Si-Si.

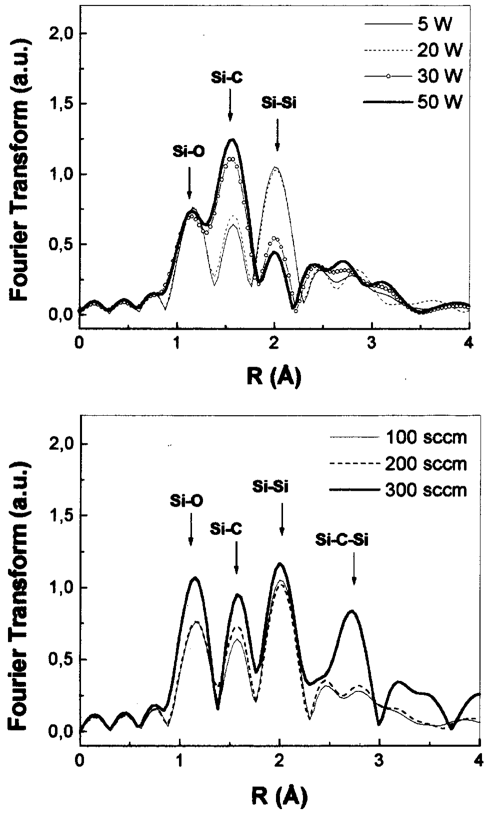

Figure 6. Fourier transform for (a) the power variation series and (b) the H_2 dilution variation series.

Fig. 6a shows the Fourier transform of the EXAFS spectra of the samples grown with different RF power. It is observed that samples grown with higher RF power exhibit a larger area under the peak associated to the Si-C coordination. Fig. 6b shows the Fourier transform of the EXAFS spectra of samples deposited under different H_2 dilution, at low RF power density (12.5mW/cm^2). The data reveal that the sample deposited at the highest H_2 dilution (300 sccm) presents a medium range order structure, with distances greater than 3 Å, related to the second coordination shell.

The coordination for the Si-C bond increased for increasing RF power from 1.65, for sample deposited at 12.5 mW/cm^2, to 2.8 for the sample deposited at 125 mW/cm^2. For all samples the total Si coordination was greater than 3.5

III.2. Doping

The electrical measurements on n-type doped samples confirm that the "starving plasma" condition has a very important effect on the doping properties of a-SiC:H. Fig. 7 shows the Arrhenius plots for samples grown in "starving" and "non-starving" plasma condition and implanted with 3.10^{20} cm^{-3} nitrogen and phosphorus.

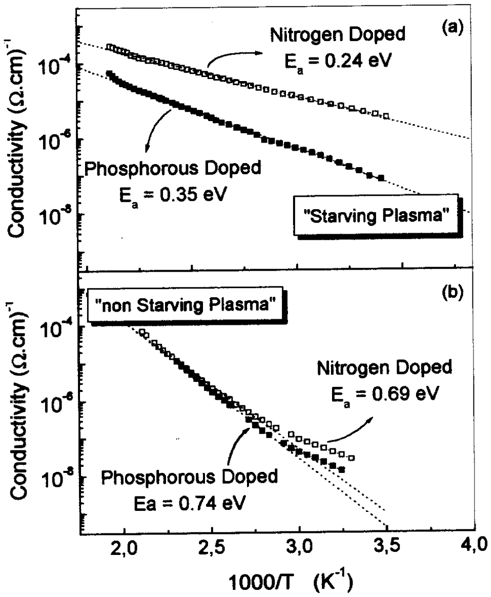

Figure 7. Arrhenius plots for nitrogen and phosphorous doped sample grown in (a) "starving" plasma condition and (b) "non-starving" plasma condition. In both cases the impurity concentrations is 10^{20} cm^{-3}.

It is observed that the sample obtained in "starving plasma" shows an activation energy of 0.24 eV, which is not only a low value but 3 times lower than the exhibited by the sample grown in "non-starving plasma" conditions. Note that this behavior is observed for both doping elements, phosphorus and nitrogen, and that nitrogen appear as a much more efficient doping impurity than phosphorus.

The results for samples grown in the silane starving plasma condition and implanted with 10^{20} and 10^{21} cm^{-3} nitrogen and phosphorous are depicted in Fig. 8. For comparison the electrical conductivity for intrinsic a-SiC:H is included. As we can see, the results for an impurity concentration of 10^{21} cm^{-3} are very encouraging, presenting an activation energy as low as 0.12 eV and room temperature dark conductivity in the order of 10^{-3} (Ω.cm)$^{-1}$. It should be pointed out that the "starving plasma" condition improves the n-type doping efficiency of the films up to levels close to those obtained in device quality a-Si:H.

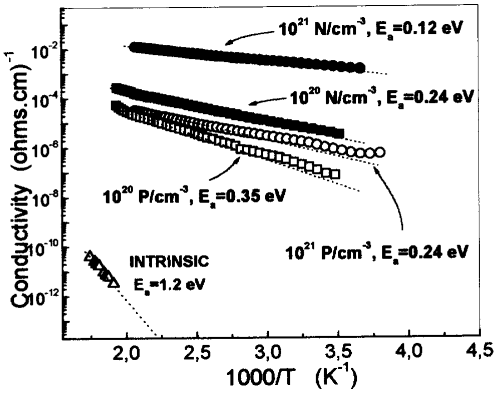

Figure 8. N-type doping: Arrhenius plot for stoichiometric samples grown in "starving plasma" condition implanted with 10^{20} and 10^{2l} cm^{-3} nitrogen (solid symbol) and phosphorus (open symbol).

Table 2: Room temperature electrical conductivity (σ_{RT}), conductivity therrnal activation energy (E_a) and the optical (E_o) for the Al diffused samples.

Diffusion Process	σ_{RT} $(\Omega.cm)^{-1}$	E_a (eV) ± 0.05	E_o (eV) ± 0.2
Intrinsic	$< 10^{-15}$	1,2	2,6
350 °C, 4 h	$\sim 5 \times 10^{-15}$	0.86	2,6
350 °C, 8 h	$\sim 5 \times 10^{-15}$	0.9	2,6
350 °C, 12 h	$\sim 5 \times 10^{-15}$	0.8	2,6
Intrinsic	$< 10^{-15}$	1.1	2.6
450 °C, 2 h	3×10^{-12}	0.39	-
450 °C, 4 h	8×10^{-12}	0.35	-
450 °C, 6 h	3×10^{-11}	0.38	-
450 °C, 6 h	10^{-7}	0.17	-

Also, it is observed that sample doped with 10^{21} cm^{-3} phosphorus has almost the same activation energy than sample doped with 10^{20} cm^{-3} nitrogen, but exhibits a conductivity significantly lower, indicating that the mobility for nitrogen doped samples is higher.

As it can be appreciated in Table 2, the aluminum diffusion had a clear effect in the transport characteristics of the samples. It is also observed that the optical gap remained unchanged for all samples. The Arrhenius plot for the aluminum diffused samples is depicted on Fig. 9.

As we can see, the doping was effective, leading to an activation energy of ~0,2 eV in the best case, which is very low if we consider that the energy gap of the samples is 2,4 eV and that we are dealing with an amorphous alloy, where it is normally difficult to shift the Fermi level position. Despite the low activation energy, the electrical conductivity remains quite low, being $\sim 10^{-7} (\Omega.cm)^{-1}$ at room temperature and $\sim 10^{-6} (\Omega.cm)^{-1}$ at 570 K. Probably this fact is related with a non-ohmic character of the metal contacts. It is known that obtaining good ohmic contacts to p-type SiC is a very difficult task, even for crystalline material, and specially for lower doping concentrations. This problem makes difficult to obtain reproducible results, specially for the absolute value of the dark conductivity, since the contribution of the contact resistance is not well evaluated. It is important to recall here that, in general, the task of high conductive p-type doping and confident metal contacts to crystalline SiC has not yet been solved [16]. In this way, the results reported here with Al doping are very promising.

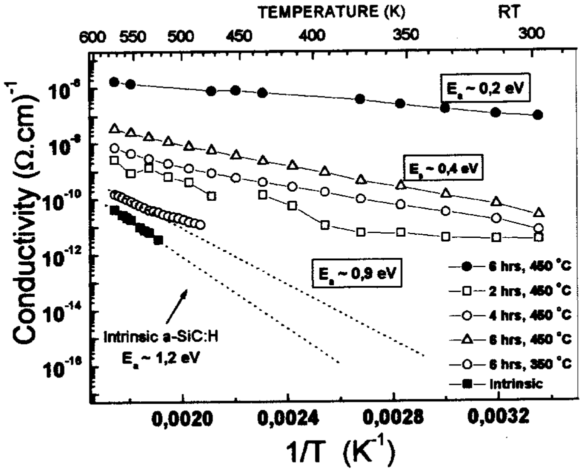

Figure 9. Conductivity vs. 1/T for intrinsic and Al doped samples. The data are fitted with functions $\ln \sigma = A^i + B^i/T$ where i is □, ○, ●, ■. The activation energies are the slopes of those functions.

IV Conclusions

The results obtained for silicon carbon alloys have indicated the way to produce a highly ordered material and the trend to obtain microcrystalline SiC by PECVD.

This fact is well illustrated in Fig. 10 which shows the FTIR spectrum for a sample crystallized at 1200 ^{o}C (crystallized SiC sample) together with the spectra of three close to stoichiometry a-SiC:H as deposited samples, grown in the following conditions: (a) out of the "silane starving regime" ("non-starving" sample), (b) in "silane starving" conditions ("starving" sample) and (c) in "silane starving" conditions with hydrogen diluted gas mixture ("starving"+H_2 sample). It is observed that the crystallized sample exhibits a single peak spectrum, just one band at 800 cm^{-1}, corresponding to Si-C vibrations. The "starving"+H_2 sample exhibits a large Si-C stretching band and a very small Si-H stretching band. In fact, the spectrum is very close to that of the crystallized sample, the main difference being the full width at half maximum, due to the structural disorder. This indicates that the short range order of our material is very similar to crystalline SiC, in other words, we have attained our goal of producing the amorphous counterpart of c-SiC.

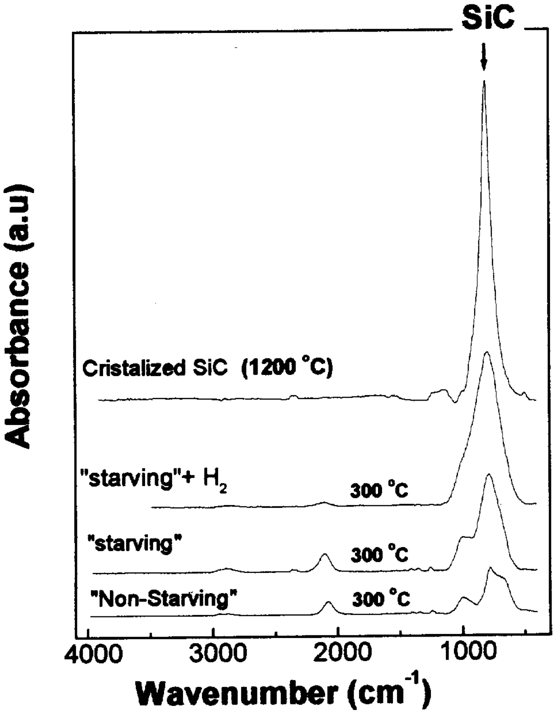

Figure 10. FTIR spectra for 3 as deposited samples (300 °C) and one thermally crystallized at 1200°C.

On the other hand, the "non-starving" sample presents just a small SiC peak and exhibits quite large bands corresponding to Si-H_n (640 and 2090 cm^{-1}) and Si-CH_3 vibrations (1250 cm^{-1}). On the contrary, the "starving" sample already presents the main features of silicon carbide materials, this is to say a large Si-C stretching band, but still presents a large band due to Si-H_n bonds and some Si-CH_3 vibrations, the CH_n vibrations in the 2900cm^{-1} spectral region are also apparent.

These FTIR results are corroborated by the EXAFS experiments which lead to an increased coordination number for Si-C bonds for higher RF power densities, signature of a higher degree of short range order. In this way it was demonstrated that conventional PECVD technique can be used successfully to produce amorphous silicon carbon alloys with excellent structural properties provided that a set of deposition parameters, which enable to control the plasma chemistry, are established.

It was also shown that the "starving plasma" condition has indeed an important role in increasing the n-type doping efficiency of PECVD produced a-SiC:H since a sample implanted with a nitrogen dose of 10^{20} cm^{-3} grown in "non-starving" conditions showed an activation energy much higher than a "starving" produced sample implanted with the same dose. Furthermore, for a sample grown in this condition, activation energy and dark conductivity values comparable to device quality a-Si:H were obtained. It is also demonstrated that nitrogen doping is more efficient than phosphorus doping for these a-$Si_{1-x}C_x$ alloys. The experiments with low temperature thermal diffusion of Al resulted in a very promising shift of the Fermi level. The electrical conductivity however, must be increased and for this purpose it is important to prepare ohmic contacts and decrease the contact resistivity.

Acknowledgements

The authors are grateful to Dr. M.H. Tabanicks for the RBS and FRS measurements. This work was partially supported by the Brazilian agencies: FAPESP, CNPq and CAPES.

References

[1] J. Bullot and M.P. Schmidt, Phys. Stat. Sol. (b) **143**, 345 (1987).

[2] R. S. Sussman and R. Odgen, Phil. Mag. B **44**, 137 (1981).

[3] I. Solomon, M. P. Schmidt and H. Tran-Quoc, Phys. Rev. B **38**, 9895 (1988).

[4] V. Mastelaro, A.M. Flank, M.C.A. Fantini, D.R. Bittencourt, M.N.P. Carreño and I. Pereyra, J. Appl. Phys. **79**, 1324 (1996).

[5] I. Pereyra and M.N.P. Carreño, Journal of Non-Cryst. Solids **201**, 110 (1996).

[6] I. Pereyra, M.N.P. Carreño, R.J. Prado, D.R.S. Bittencourt, M.H. Tabacniks and M.C.A. Fantini, J. Appl. Phys. **84**, 2371 (1998).

[7] H. Wieder, M. Cardona and C.R. Guarnieri, Phys. Status Solidi B **92**, 99 (1979).

[8] F. Evangelisti, J. of Non-Cryst. Sol. **164-166**, 1009 (1993).

[9] C.C. Tsai, G.B. Anderson and R.Thompson, Mat. Res. Soc. Symp. Proc. **192**, 475 (1990).

[10] Y. Hamakawa, D. Kruangam, T. Toyama, H. Yoshimi, S. Paasche and H. Okamoto, Optoelectronics **4**, 281 (1989).

[11] G. Ganguly, S. C. DE, Swati Ray and A. K. Barua, J. of Non-Crys. Sol. **114**, 822 (1989).

[12] M.N.P. Carreño, J.P. Bottecchia, I. Pereyra, Thin Solid Films **308-309**, 219 (1997).

[13] M.N.P. Carreño, I. Pereyra and H.E.M. Peres, J. of Non-Cryst. Sol. **227-230**, 483 (1998).

[14] R.J. Prado, D.R.S. Bittencourt, M.H. Tabackniks, M.C.A. Fantini, M.N.P. Carreño and I. Pereyra, J. Appl. Cryst. **30**, 659 (1997).

[15] G.S. Cargill III and F. Spaepen, J. of Non-Cryst. Solids **43**, 91 (1981).

[16] J. Crofton, L.M. Porter and J.R. Williams, Phys. Stat. Sol. (b) **202**, 581 (1997).